Cool- and Warm-Season Precipitation Reconstructions over Western New Mexico

D. W. STAHLE,* M. K. CLEAVELAND,* H. D. GRISSINO-MAYER,+ R. D. GRIFFIN,# F. K. FYE,* M. D. THERRELL,@ D. J. BURNETTE,* D. M. MEKO,# AND J. VILLANUEVA DIAZ&

* *Department of Geosciences, University of Arkansas, Fayetteville, Arkansas*
+ *Department of Geography, University of Tennessee at Knoxville, Knoxville, Tennessee*
@ *Laboratory of Tree-Ring Research, The University of Arizona, Tucson, Arizona*
# *Department of Geography, Southern Illinois University at Carbondale, Carbondale, Illinois*
& *Instituto Nacional de Investigacioones Forestales, Agricolas, y Pecurarias, Centro Nacional de Investigacion Disciplinaria en Relacion Agua-Suelo-Planta-Atmosfera, Gomez Palacio, Durango, Mexico*

(Manuscript received 28 July 2008, in final form 3 December 2008)

ABSTRACT

Precipitation over the southwestern United States exhibits distinctive seasonality, and contrasting ocean–atmospheric dynamics are involved in the interannual variability of cool- and warm-season totals. Tree-ring chronologies based on annual-ring widths of conifers in the southwestern United States are well correlated with accumulated precipitation and have previously been used to reconstruct cool-season and annual precipitation totals. However, annual-ring-width chronologies cannot typically be used to derive a specific record of summer monsoon-season precipitation. Some southwestern conifers exhibit a clear anatomical transition from the earlywood and latewood components of the annual ring, and these exactly dated subannual ring components can be measured separately and used as unique proxies of cool- and warm-season precipitation and their associated large-scale ocean–atmospheric dynamics. Two 2139-yr-long reconstructions of cool- (November–May) and early-warm season (July) precipitation have been developed from ancient conifers and relict wood at El Malpais National Monument, New Mexico. Both reconstructions have been verified on independent precipitation data and reproduce the spatial correlation patterns detected in the large-scale SST and 500-mb height fields using instrumental precipitation data from New Mexico. Above-average precipitation in the cool-season reconstruction is related to El Niño conditions and to the positive phase of the Pacific decadal oscillation. Above-average precipitation in July is related to the onset of the North American monsoon over New Mexico and with anomalies in the 500-mb height field favoring moisture advection into the Southwest from the North Pacific, the Gulf of California, and the Gulf of Mexico. Cool- and warm-season precipitation totals are not correlated on an interannual basis in the 74-yr instrumental or 2139-yr reconstructed records, but wet winter–spring extremes tend to be followed by dry conditions in July and very dry winters tend to be followed by wet Julys in the reconstructions. This antiphasing of extremes could arise from the hypothesized cool- to early-warm-season change in the sign of large-scale ocean–atmospheric forcing of southwestern precipitation, from the negative land surface feedback hypothesis in which winter–spring precipitation and snow cover reduce surface warming and delay the onset of the monsoon, or perhaps from an interaction of both large-scale and regional forcing. Episodes of simultaneous interseasonal drought (''perfect'' interseasonal drought) persisted for a decade or more during the 1950s drought of the instrumental era and during the eighth- and sixteenth-century droughts, which appear to have been two of the most profound droughts over the Southwest in the past 1400 yr. Simultaneous interseasonal drought is doubly detrimental to dry-land crop yields and is estimated to have occurred during the mid-seventeenth-century famines of colonial New Mexico but was less frequent during the late-thirteenth-century Great Drought among the Anasazi, which was most severe during the cool season.

1. Introduction

The precipitation climatology of the southwestern United States includes a summer maximum in convective precipitation associated with the northward penetration of the North American Monsoon System (NAMS) and a weaker winter–spring maximum associated with

Corresponding author address: Dr. David W. Stahle, Department of Geosciences, University of Arkansas, Ozark Hall 113, Fayetteville, AR 72701.
E-mail: dstahle@uark.edu

DOI: 10.1175/2008JCLI2752.1

the southward depression of the Pacific storm track. The interannual to decadal variability of winter precipitation over this region has been linked with equatorial and North Pacific sea surface temperatures (SSTs) associated with the El Niño–Southern Oscillation (ENSO; Ropelewski and Halpert 1987) and the Pacific decadal oscillation (PDO; Zhang et al. 1997) through Rossby wave teleconnnections, changes in the mean storm track (Sheppard et al. 2002), and by the tropical modulation of midlatitude eddies (Seager et al. 2003, 2005; Herweijer et al. 2006). Summer precipitation over the Southwest is linked with continental-scale atmospheric circulation changes from the winter to summer season associated with the development of the NAMS, including the strength and position of the subtropical ridge over western North America during the warm season, land surface heating across Mexico and the Southwest, a shift from mean westerly to southerly wind flow, and the advection of moisture from the Pacific Ocean, the Gulf of California (GOC), and the Gulf of Mexico (Carleton 1987; Douglas et al. 1993; Adams and Comrie 1997; Grantz et al. 2007).

The interannual to decadal variability of Southwestern summer precipitation and in the larger North American monsoon system have been related to the Pacific–North America pattern (PNA; Carleton et al. 1990), ENSO (Higgins et al. 1999), PDO (Castro et al. 2001), the combined interannual and interdecadal modes of SST variability over the Pacific (Castro et al. 2007), the Atlantic multidecadal oscillation (AMO; Wang 2007), SST anomalies in the Western Hemisphere warm pool (WHWP; Wang and Enfield 2003), and land surface feedbacks associated with winter–spring precipitation and snowpack over western North America (Gutzler 2000; Higgins and Shi 2000; Grantz et al. 2007). In spite of these associations, prospects for the predictability of summer precipitation over the NAMS region may be low (Nicholas and Battisti 2008). However, linear forecasts of monsoon onset over Arizona and New Mexico based on winter and spring SSTs over the Pacific have produced modest results (Higgins and Shi 2000), and the conditional probability of summer precipitation does appear to be related to the timing of monsoon onset (Higgins et al. 1999). Pan-Pacific SSTs during the boreal summer have also been related to early summer precipitation over the Southwest and may prove useful for seasonal prediction at monsoon onset (Castro et al. 2007). Mitchell et al. (2002) identify a GOC SST threshold of >26°C needed for the onset of monsoon precipitation, and most of the summer precipitation [June–September (JJAS)] over Arizona and New Mexico occurs after GOC SSTs exceed 29°C. Finally, cool-season precipitation and snow cover have also been linked with subsequent summer precipitation (Gutzler 2000; Higgins and Shi 2000; Zhu et al. 2005), especially early in the monsoon season (Grantz et al. 2007), and may provide a basis for conditional forecasts. Evidence for the occasional influence of antecedent precipitation on summer rains over the Southwest is limited in the short instrumental record (e.g., Gutzler 2000) but may exist in tree-ring proxies of seasonal precipitation totals.

Some of the longest and most climatically sensitive tree-ring chronologies have been developed from arid-site conifer species in the southwestern United States and northern Mexico. These tree-ring data have a long history of climate and hydrological applications, including estimates of past drought (Douglass 1920; Meko et al. 1980), streamflow (Schulman 1945; Stockton 1975; Hidalgo et al. 2000; Woodhouse et al. 2005; Meko et al. 2007), annual precipitation (Grissino-Mayer 1995), winter precipitation (D'Arrigo and Jacoby 1991; Cleaveland et al. 2003; Villanueva-Diaz et al. 2007), Palmer drought severity indices (PDSIs; Cook et al. 2007), atmospheric circulation patterns (Fritts 1966), and indices of large-scale ocean–atmospheric forcing (Lough and Fritts 1985; Biondi et al. 2001; Stahle et al. 1998; Gedalof and Smith 2001). These exceptional proxy tree-ring chronologies in some cases have explained over 70% of the interannual variability in streamflow and PDSIs over portions of the Southwest.

Analyses of the monthly climate response indicate that the strongest seasonal climate signal encoded in the annual rings of Southwestern trees comes primarily during the winter and spring, when winter storms deliver the soil moisture that subsequently sustains radial tree growth during the spring and early summer (Fritts 1966, 2001). Ironically, little success has been reported in attempts to separately reconstruct warm-season precipitation even though summer rains can raise rates of net photosynthesis (Fritts 1966). The continent-wide summer PDSI reconstructions of Cook et al. (2004; summer = JJA average) integrate temperature and precipitation influences on soil moisture for several months during and preceding the summer season and do not provide an unambiguous history of summer precipitation associated with the NAMS. In fact, few, if any, of the routinely developed total-ring-width (TRW) chronologies in the American Southwest and northern Mexico provide a strong and unique record of summer precipitation. This has limited the application of total-ring-width chronologies to the reconstruction of climate and environmental conditions during the warm season, including the water budget and chemistry of western lakes (Benson 2003), the NAMS (Meko and Baisan 2001; Therrell et al. 2002), and crop yields (Burns 1983). The

hypothesized Anasazi abandonment of large areas of the Colorado Plateau during the thirteenth-century ''Great Pueblo Drought'' (Douglass 1935) has been criticized on the grounds of the ambiguous summer precipitation signal in these conifer chronologies (Burns 1983). Winter–spring drought clearly prevailed during this late-thirteenth-century episode (Cook et al. 2007; Benson et al. 2007; Stahle and Dean 2009), but the correlation between winter–spring precipitation and subsequent summer rainfall over the Colorado Plateau is weak and winter drought may not have prevented crop production if the summer rains did not also fail. The reconstruction of an independent summer precipitation history could help test the drought-abandonment hypothesis and would provide a unique long-term perspective on the variability and forcing of the summer monsoon over the Southwest.

The annual growth rings of many southwestern conifers exhibit a distinctive anatomical transition from the spring to summer seasons, referred to as the earlywood (EW) and latewood (LW) components of the annual ring (or springwood and summerwood, respectively). These exactly dated annual-ring components can be measured separately (e.g., Schulman 1942; Cleaveland 1975) and used as unique proxies of both precipitation during the cool and warm season and the distinctive large-scale ocean–atmospheric dynamics associated with climate variability in each season (Meko and Baisan 2001; Therrell et al. 2002). The transition between EW and LW is often abrupt, reflecting the rapid decrease in cell size and lumen area, and usually appears as an obvious color change within the annual ring. The change from EW to LW can be measured objectively, with X-ray densitometry as a threshold in wood density, or optically, at the first cellular evidence for latewood formation.

We have developed new EW and LW width chronologies from ancient Douglas-fir (*Pseudotsuga menziesii*) and ponderosa pine (*Pinus ponderosae*) trees and relict wood collected in 1992 (Grissino-Mayer 1995) and subsequently in 2004 at El Malpais National Monument in west-central New Mexico (Fig. 1). These two time series are both 2139 yr long and are among the longest precipitation-sensitive tree-ring chronologies yet developed for the American Southwest (e.g., Salzer and Kipfmueller 2005). We hypothesize that the EW and LW chronologies from El Malpais can be used to develop separate reconstructions of winter and summer precipitation over northwestern New Mexico and provide insight into the long-term variability and forcing of these distinctive seasonal precipitation regimes.

In this paper we describe the ancient forests found on the barren lava fields at El Malpais National Monument. We document the climate signal in EW and LW width chronologies and use them to separately reconstruct winter (November–May season) and summer precipitation (July only) over northwestern New Mexico. The ocean–atmospheric and land surface forcing of observed and reconstructed precipitation are described for each season. We compare the cool- and warm-season precipitation reconstructions and identify decade-long episodes of simultaneous drought during the winter–spring and early summer. Simultaneous interseasonal drought could have a negative impact on dry-land crop yields (''perfect drought''), and episodes of simultaneous wetness during both seasons (''perfect pluvial'') would favor dry-land crop yields. Statistically significant antiphasing between cool- and early-warm-season precipitation extremes is also detected in the reconstructions and may be related to regional and/or large-scale climate forcing. Finally, we map the seasonal response of selected earlywood and latewood width chronologies to highlight the potential for cool- and warm-season precipitation reconstructions across the North American monsoon region.

2. Study area

The unique vegetation communities found on the lava flows at El Malpais were first described by Lindsey (1951), including the stunted slow-growing conifers. The sparsely vegetated and forbidding lava-rock terrain has been protected from grazing, logging, and other human impacts (Fig. 1). Consequently, some of the oldest trees known in the American Southwest have been found in pristine woodland communities at El Malpais (Grissino-Mayer et al. 1997). The paleoclimatic significance of these trees was proven by Grissino-Mayer (1995), who used total ring width to reconstruct annual precipitation totals in New Mexico for over 2100 yr. This was the longest directly calibrated and verified reconstruction in the American Southwest, and it documented major ''megadroughts'' in the eighth and sixteenth centuries (Grissino-Mayer 1995; Stahle et al. 2000a). This exceptionally long chronology utilized core samples from ancient living trees and cross sections cut from well-preserved remnant wood still found littering the rugged fire-protected basalt fields (Fig. 1).

3. Data and methods

a. Instrumental climate data

Individual weather recording stations are sparsely distributed in west-central New Mexico. The nearest weather stations to the monument are located at El Moro National Monument and Grants (both over 30 km from

FIG. 1. A dead Rocky Mountain Douglas-fir at El Malpais National Monument, New Mexico. Living Douglas-fir trees exceeding 1200 yr old and relict wood persisting for centuries have been found on the rugged basalt fields at El Malpais.

the tree-ring site), with daily precipitation observations beginning in 1948 and 1953, respectively. However, the National Oceanic and Atmospheric Administration (NOAA) climate division data provide a reasonable record of monthly precipitation totals over the region beginning in 1931 (Fig. 2; Karl et al. 1983). We used the precipitation data averaged among New Mexico climate divisions 1 and 4 (the northwest and west-central mountain regions, respectively) for the winter and summer precipitation reconstructions reported below. The mean monthly precipitation totals for the average of climate divisions 1 and 4 are presented in Fig. 3, illustrating the strong summer and weak winter maxima in precipitation over the El Malpais region.

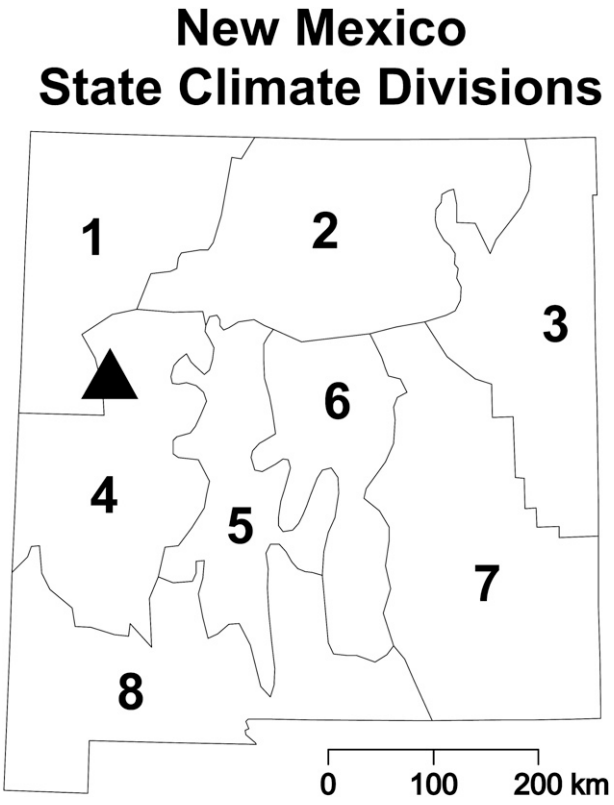

FIG. 2. The location of El Malpais is indicated (triangle), along with the boundaries of the eight climate divisions in New Mexico. Monthly precipitation was averaged between divisions 1 and 4 for this study, but the EW and LW width chronologies from El Malpais are significantly correlated with seasonalized precipitation (November–May and July, respectively) for all divisions in New Mexico but 3 and 7.

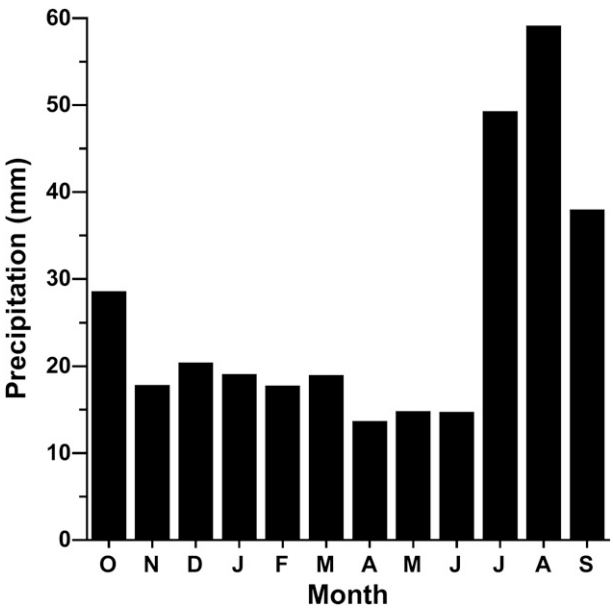

FIG. 3. The monthly precipitation averages for New Mexico climate divisions 1 and 4 (combined) are plotted for the water year, based on the 1931–2002 period. Note the dramatic onset of monsoonal precipitation in July, the summer precipitation maxima (July–September), and the modest secondary peak in winter precipitation (December–March).

The gridded monthly SST data for the global oceans (Kaplan et al. 1997) and 500-mb geopotential height anomalies (Kalnay et al. 1996) were used to identify large-scale SST and atmospheric circulation influences on observed and reconstructed precipitation over northwestern New Mexico during the winter and summer seasons. The possible link between wet winter–spring extremes and subsequent July precipitation was tested with contingency table analyses of the reconstructions.

b. Seasonal climate signal in earlywood and latewood chronologies

The lack of a routine summer precipitation signal in TRW chronologies of conifers in the arid Southwest simply reflects the fact that most of the annual ring is formed as earlywood during the spring and early summer. For samples of Douglas-fir from three sites on the Colorado Plateau, the earlywood component represented 75.5% of the annual-ring width and 24.5% was latewood (Cleaveland 1983). At El Malpais, the LW component averages only 20.0% of the total ring width.

Although the latewood represents a fraction of the total ring width, it is formed during summer conditions (Fritts 1966) and might be used to provide estimates of summer precipitation and the onset phase of the NAMS (Meko and Baisan 2001; Therrell et al. 2002). Most previous dendroclimatic studies in the Southwest have used total ring width as the predictor and have produced high-quality reconstructions of winter–spring precipitation (e.g., D'Arrigo and Jacoby 1991; Salzer and Kipfmueller 2005), ''summer PDSI'' (JJA average, integrating climate over the winter–spring–summer seasons; Cook et al. 2004), and annual precipitation (Rose et al. 1981; Grissino-Mayer 1995). However, the total-ring-width proxy is heavily influenced by climate conditions during and preceding the spring growing season and does not record an unbiased history of summer rainfall or the NAMS.

In many cases, but certainly not all, EW and LW can be quickly and objectively measured using simple optical criteria on a stage micrometer, and separate seasonal tree-ring chronologies of EW and LW width can be directly computed from the same trees. The Douglas-fir and ponderosa pine are ''abrupt transition'' species (Panshin and de Zeeuw 1970) and the EW and LW components of the annual ring can be discriminated

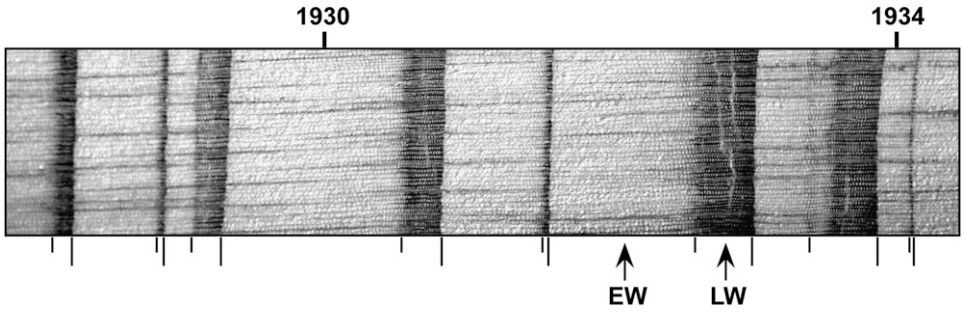

FIG. 4. A sequence of annual growth rings for a Douglas-fir specimen from El Malpais is illustrated from 1927 to 1935 (radial growth advances from left to right). Note the light-colored earlywood and dark-colored latewood cells formed during the spring and summer, respectively. (bottom) The intra-annual ring boundaries between EW and LW are marked with short lines and the interannual ring boundaries are marked with long lines. Note the high variability of EW, LW, and total ring width and the false ring in 1933. The rings for 1929 and 1934 both included narrow EW but very different LW widths, illustrating some independence between EW and LW width and winter–spring vs summer precipitation over New Mexico.

visually by the sudden change in cell size, lumen size, and color (Fig. 4). But even in abrupt transition species, the shift from EW to LW can sometimes occur over several cells. The transition can also be complicated by the formation of false rings (i.e., LW cells in the EW or EW cells in the LW). We have therefore adopted three simple optical criteria to separate and measure the EW and LW components of annual rings in conifers from the American Southwest and Mexico (Stahle et al. 2000b; Therrell et al. 2002; Villanueva-Diaz et al. 2007):

1) When the boundary between EW and LW is abrupt, the measurement is made at that boundary.
2) When there is a gradual transition from the EW to LW component of the annual ring, the zones of pure EW and pure LW are identified and the measurement is made halfway between those pure zones.
3) When there is a false ring, the measurement is made at the first onset of lumen contraction (i.e., all false rings are measured as part of the LW).

c. *Tree-ring chronology development*

We measured EW and LW width on the dated tree-ring collections from El Malpais developed by Grissino-Mayer (1995). We also revisited the monument in 2004 and collected core samples from additional living trees to update the chronology. All specimens were highly polished and visually cross dated under the microscope using the Douglass method of cross dating (Douglass 1941; Stokes and Smiley 1996). The dated tree rings were measured to 0.001 mm, which is necessary to define the variability of the minute LW width in these slow-growing arid-site conifers with adequate precision. The accuracy of tree-ring dating and measurement for both the EW and LW time series from each tree was then checked and confirmed with the quality-control program COFECHA (Holmes 1983; Grissino-Mayer 2001).

The EW and LW width chronologies were computed as the robust mean value of the normalized, detrended, and standardized EW and LW widths available each year, using the computer programs ARSTAN (Cook 1985; Cook and Holmes 1986; information available online at http://www.ldeo.columbia.edu/res/fac/trl/public/publicSoftware.html) and CHRONOL (information available online at http://www.ltrr.arizona.edu/software.html). The EW and LW width time series were normalized prior to detrending to better cope with the large differences in variance typical of the LW width series. Detrending attempts to remove nonclimatic changes in mean ring width associated with the increasing size and age of the tree. Detrending and standardization were accomplished by fitting a smooth growth curve to the normalized EW and LW width time series from each radii and then dividing the (normalized) measured width by the value of the fitted curve at each year. Standardization produces indexed time series for all radii that have a mean of 1.0, approximately stationary variance, and can be averaged together into the mean site chronology with equal weighting.

The measurement and standardization of LW width in the slow-growing conifers from El Malpais can be challenging. Some microscopic one-cell-wide LW time series had to be excluded from the analysis because of low variability, even though they were correctly dated and the EW component from the same tree was perfectly suitable for analysis. The detrending of many LW time series was also problematic and could not be adequately modeled with negative exponential or negative

linear growth functions, which are the classical biological models invoked to describe the long-term decline in ring width due to the increasing size and age of the tree (Fritts 2001). Some LW width time series from individual trees at El Malpais are subject to rapid order-of-magnitude changes in mean LW width, but with massive replication these few problematic LW time series can be excluded from the analysis with little penalty.

After experimentation, we found that optimal detrending and standardization results were achieved for LW at El Malpais by first normalizing the raw LW width data and then fitting to each normalized LW series a cubic-smoothing spline with an amplitude of frequency response of 0.5 at a wavelength of 200 yr, which reduces the variance in a sine wave with a period of 200 yr by 25% (Cook and Peters 1981). The calculated LW width indices available at each year were averaged into the LW width index chronology using a robust mean-value function that discounts statistical outliers in the estimation of the mean (Cook 1985). For consistency, we used a 200-yr cubic-smoothing spline for all detrending and standardization of both EW and LW widths at El Malpais (i.e., standard chronologies in both cases). Modest trend in the envelope of variability was present in the derived EW and LW chronologies, related in part to changing sample size, and was stabilized using a 100-yr spline fit to the chronology variance (i.e., the spline was fit to the absolute values of the indices minus their mean, ratios of the fitted spline to the absolute values were computed, the sign was restored to the absolute values, and the mean was added back to produce the variance-stabilized chronology). Therefore, these EW and LW chronologies and their derived precipitation reconstructions are useful for exploring interannual to multidecadal variability in winter and summer precipitation over New Mexico for the past 2100 yr but cannot be used to track centennial changes.

There is strong autocorrelation in growth from earlywood to latewood in these arid-site conifers and, therefore, considerable overlap in the seasonal climate response of EW and LW, making detection of a pure summer rainfall signal not influenced by conditions earlier in the growing season quite difficult. Meko and Baisan (2001) have shown that removing the intercorrelation between EW and LW width chronologies can clarify the summer rainfall signal in chronologies of LW growth. Following Meko and Baisan (2001), we used linear regression with the LW width chronology from El Malpais as the dependent variable and the EW width chronology as the independent variable (after all normalization, detrending, standardization, and variance adjustment; Fig. 5). There is large variability around this linear regression fit between LW and EW growth

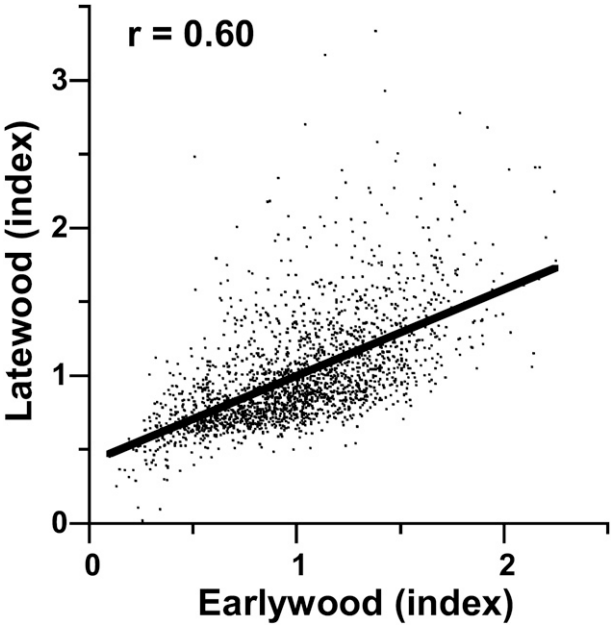

FIG. 5. This scatterplot illustrates the regression of LW width on EW width for the 2139-yr-long chronologies from El Malpais, New Mexico. The residuals from this regression, LW_{adj}, were used to model the precipitation response of latewood and to reconstruct July precipitation over western New Mexico.

($R^2 = 0.36$), but the explained variance did not change significantly when the relationship was modeled with a polynomial function (for a seventh-order polynomial, $R^2 = 0.366$). The residuals from the bivariate regression are referred to as the adjusted latewood chronology (LW_{adj}) and were used for modeling the monthly precipitation response. By definition, the LW_{adj} width chronology is uncorrelated with the EW chronology and should be useful for detecting a separate warm-season precipitation signal.

4. Results

a. The earlywood and latewood width chronologies from El Malpais

The EW and LW width chronologies are well replicated for the outer 1300 yr and extend continuously between 137 B.C. and A.D. 2004, for a total of 2139 yr. The EW width chronology is based on 119 radii from 61 separate trees, and the LW chronology is based on 109 radii from 55 trees. Fewer trees and radii were included in the LW width chronology because of the microscopic, low-variability LW growth recorded by some trees at El Malpais, often involving only one xylem cell in the slowest growing cases. The sample size in both the EW and LW chronologies is highest in the twentieth century (up to 66 and 50 radii, respectively), exceeds 10 radii

after A.D. 664, and declines to only 1 radius for 46 yr during the fourth and fifth centuries (A.D. 457–502) and to 4 radii from one tree before A.D. 102. We are nevertheless certain of the calendar-year dating during the entire 2139-yr-long series, including the poorly replicated portions of the chronology, by virtue of the cross dating with other long tree-ring chronologies in the region (Grissino-Mayer 1995). For this reason, we present the entire 2139-yr-long reconstructions but note that the severity and persistence of droughts and pluvials during periods of low sample size will be subject to change with improved replication.

The strength of the common signal in the interannual variability of EW and LW width is remarkably high in the trees and radii included in the chronologies at El Malpais. The average interseries correlation computed with the program COFECHA (Holmes 1983; Grissino-Mayer 2001) was $r = 0.87$ ($P < 0.0001$) for the entire collection of EW time series and $r = 0.61$ ($P < 0.001$) for the LW time series. This strong internal agreement among the individual trees and radii incorporated into the final mean index chronologies reflects the shared seasonal climate influence on EW and LW formation and endorses the use of simple optical criteria for the measurement and development of EW and LW width chronologies in these Southwestern arid-site conifers (other key chronology statistics include mean sensitivities of 0.38 and 0.24 and first-order autocorrelations of 0.18 and 0.32 for the EW and LW chronologies, respectively).

b. *Seasonal precipitation response of earlywood and latewood width at El Malpais*

To define the seasonal precipitation response of the EW, LW, and LW_{adj} width chronologies, the monthly precipitation totals for New Mexico climate divisions 1 and 4 were first averaged into a ''northwestern'' New Mexico regional record (Figs. 2, 3). Each chronology type was then correlated with the monthly precipitation totals over the water year (previous October through current September) and the correlation coefficients are plotted in Fig. 6. The EW width chronology is significantly and positively correlated with monthly precipitation averaged over northwestern New Mexico during the cool season, from November through May (Fig. 6). The LW width chronology is positively correlated with spring–summer precipitation totals, significantly ($P < 0.05$) for the months of April, June, and July (not shown). This overlap in the spring precipitation response between the EW and LW width chronologies is eliminated when the adjusted LW chronology is correlated with monthly precipitation and the only significant positive correlation is observed with June and July (Fig. 6), during the dramatic onset phase of summer monsoonal rainfall over New Mexico (Fig. 3). These correlation analyses are consistent with the results of Meko and Baisan (2001) and Meko et al. (2003) and indicate that a distinctive early-warm-season precipitation signal can be recovered from Southwestern conifer chronologies when the residuals from a regression of the LW on EW width chronologies are used.

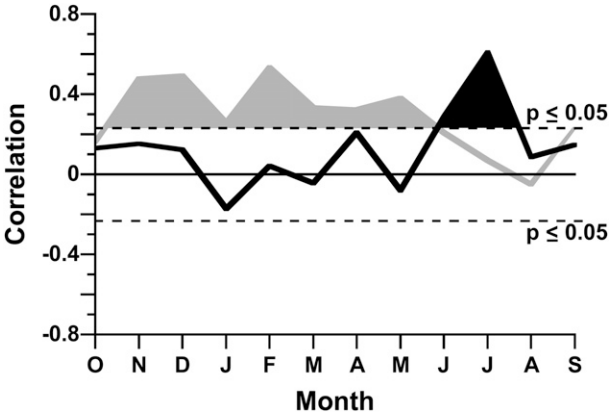

FIG. 6. The correlation coefficients computed between the EW and LW_{adj} width chronologies from El Malpais and monthly precipitation for New Mexico climate divisions 1 and 4 are plotted for the water year (1931–2002 period). EW and LW growth typically occurs during the spring and summer (April–August). Note that the EW chronology is significantly correlated with precipitation over the winter–spring (November–May; gray line) and that the LW_{adj} chronology is significantly and positively correlated with June and July (black line), not with monthly precipitation totals during the preceding spring. Note also that the LW_{adj} chronology is not significantly correlated with August or September precipitation, which are part of the summer precipitation maximum over New Mexico.

c. *Calibration and verification of the winter and summer precipitation reconstructions*

Winter–spring precipitation (November–May) was seasonalized using the average of climate divisions 1 and 4, because the EW width chronology is significantly correlated with precipitation during these months. Forward stepwise regression was used to derive a transfer function [Eq. (1)] for reconstructing November–May precipitation from the EW width chronology. Five potential predictors were derived by lagging and leading the EW chronology by 2 yr (i.e., EW width in years t_{-2}, t_{-1}, t, t_{+1}, and t_{+2}). The stepwise procedure selected years t and t_{+1}, but the addition of the t_{+1} predictor raised the adjusted R^2 negligibly (from 0.49 to 0.50) and the b_2 coefficient was not significantly different from zero. The calibration of the EW width chronology with winter–spring precipitation was therefore based on the following bivariate function for the period of 1960–2002:

TABLE 1. Calibration and verification statistics are listed for the seasonal reconstructions of total precipitation (mm) in New Mexico climate divisions 1 and 4.

Season	Calibration			Verification				
	Period	$R^2_{adj.}$[a]	Residual $r - 1$[b]	Period	r[c]	t test[d]	Sign test[e] (hit/miss)	RE/CE[f]
Nov–May (winter–spring)	1960–2002	0.49	0.25[g]	1931–59	0.73[h]	1.65[i]	23/6[j]	0.50/0.49
Jul (summer)	1960–2002	0.44	0.16[i]	1931–59	0.45[h]	−0.24[i]	14/15[i]	0.21/0.18

[a] R^2 adjusted downward for loss of degrees of freedom (Draper and Smith 1981).
[b] Autocorrelation of the residuals from regression, tested with the Durbin–Watson statistic (Draper and Smith 1981). Failure to reject the null hypothesis of no autocorrelation indicates that the residuals occur randomly, an indication that the regression model is valid.
[c] r = The Pearson product moment correlation coefficient (Draper and Smith 1981).
[d] Paired observation t test of equality of means (Steel and Torrie 1980). Note that no significant difference is the desired result.
[e] Signs of departures from the mean of each series (Fritts 2001). Means are subtracted from each series and the residuals are multiplied. A positive product is a ''hit.'' If observed or reconstructed data lie very near the mean, the year is omitted from the test.
[f] RE = Reduction of error (Fritts 2001); CE = Coefficient of efficiency (Cook and Kairiukstis 1990). There are no formal tests of significance for these statistics, but any positive result indicates that the reconstruction contributes unique paleoclimatic information. The CE is more stringent than the RE.
[g] The Durbin–Watson statistic (Draper and Smith 1981) falls in the region of uncertainty.
[h] Significant; $p < 0.001$.
[i] Not significant (i.e., there is a greater than 5% probability that the result occurred by chance).
[j] Significant; $p < 0.01$.

$$\hat{Y}_t = 13.067 + 105.885X_t, \quad (1)$$

where $\hat{Y}_t$ is the estimated November–May precipitation total for year t (in mm) and X_t is the EW width chronology value in year t. The instrumental winter–spring precipitation data from 1931 to 1959 were withheld for independent statistical verification tests on the reconstruction. The calibration and verification statistics are presented in Table 1. The EW width chronology explains 49% of the interannual variability in November–May precipitation during the calibration period ($R^2_{adj} = 0.49$ and $P < 0.001$; adjusted downward for the loss of 1 degree of freedom). The regression residuals are weakly autocorrelated, but the Durbin–Watson statistic falls in the zone of uncertainty (Table 1). Examination of the time series of instrumental and reconstructed November–May precipitation (Fig. 7a) indicates that the EW width data more faithfully reproduce dry years rather than wet extremes (see also Fig. 7b). The distributions of the observed and reconstructed November–May precipitation are both slightly skewed by extremely wet years (Figs. 7c,d; Table 2).

The relationship between reconstructed and instrumental November–May precipitation holds up well when compared with the independent precipitation data during the verification period (1931–59; Table 1a). The two time series are still significantly correlated and the reconstruction passes the reduction of error (RE) and the coefficient of efficiency (CE) tests, indicating that the reconstruction is providing skillful estimation of the independent precipitation data (Cook and Kairiukstis 1990). However, the reconstruction seriously underestimates November–May precipitation in 1941, the wettest winter–spring over northwestern New Mexico since 1931 (Fig. 7a).

The LW_{adj} chronology is significantly correlated with June and July precipitation but has no other significant positive correlation with monthly precipitation during or preceding the growing season (Fig. 6). Forward stepwise regression was also used to calculate the transfer function between the LW_{adj} chronology and July precipitation to focus on the onset of the monsoon (i.e., June was not included, even though it is weakly correlated with LW_{adj} width). The LW_{adj} widths in year t and t_{+1} were selected but the second predictor (t_{+1}) again failed to significantly improve the model. The LW_{adj} chronology was therefore calibrated with July precipitation totals averaged for divisions 1 and 4 from 1960 to 2004 using bivariate regression:

$$\hat{Y}_t = 49.701 + 49.104X_t, \quad (2)$$

where $\hat{Y}_t$ is the estimated July precipitation total for year t (in mm) and X_t is the adjusted LW width chronology value in year t. The instrumental July precipitation data from 1931 to 1959 were withheld for independent statistical verification of the reconstruction. The calibration and verification statistics are presented in Table 1. The adjusted LW width chronology explains 44% of the interannual variability in July precipitation during the calibration period ($R^2_{adj} = 0.44$ and $P < 0.001$; adjusted downward for the loss of 1 degree of freedom). The July precipitation reconstruction does a reasonable job of estimating the wet extremes but tends to underestimate the severity of the drought extremes during the calibration and verification periods (Figs. 8a,b). The

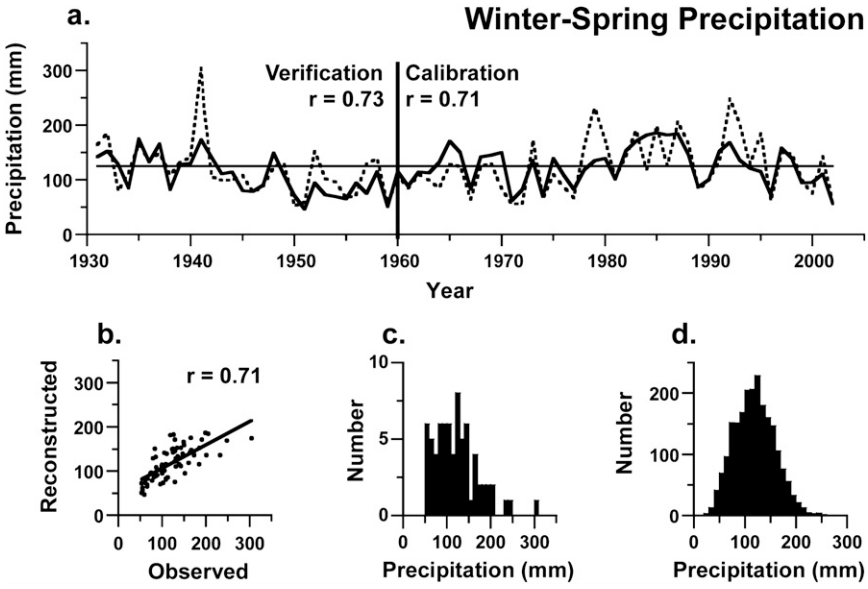

FIG. 7. (a) A time series comparison between instrumental (observed, dashed line) and reconstructed (solid line) winter–spring precipitation (November–May) for New Mexico climate divisions 1 and 4 (1931–2002). The reconstruction was based on the EW width chronology and was calibrated on the 1960–2002 period and verified by comparison with the instrumental data from 1931 to 1959. (b) The scatterplot between observed and reconstructed winter–spring precipitation illustrates the approximately linear relationship, especially during dry years. The frequency distributions of the (c) 74-yr instrumental and (d) 2139-yr reconstructed winter–spring precipitation data (statistics in Table 2).

instrumental July precipitation data are normally distributed, but the data of the July reconstruction is positively skewed by extremely wet years (Figs. 8c,d; Table 2).

The reconstruction of July precipitation passes the verification tests listed in Table 1, though not as convincingly as for the winter–spring reconstruction (including a significant correlation with instrumental July precipitation from 1931 to 1959 and positive RE and CE statistics). This may be inevitable because of the scattered nature of convective rainfall during summer, and in this study we calibrated only a single EW and single LW_{adj} chronology to prove the feasibility for long winter- and summer-season reconstructions. However, the tree-ring estimation of winter–spring and early summer precipitation can surely be improved with the development of additional millennia-long EW and LW width chronologies from the region.

5. Analysis and discussion

a. Synchronous cool- and early-warm-season drought

The cool- (November–May) and early-warm-season (July) precipitation reconstructions for western New Mexico are plotted in Fig. 9. Both reconstructions exhibit substantial interannual and decadal variability over the past 2139 yr. The two most severe and sustained cool-season droughts are estimated to have occurred in the mid-eighth and late-sixteenth centuries (Fig. 9a), consistent with the reconstruction of annual precipitation by Grissino-Mayer (1995) and using many of the same trees from El Malpais. The new cool-season reconstruction also indicates that three of the most severe and sustained droughts of the past two millennia occurred in only the last 120 yr. These three events occurred from 1891 to 1907, 1944 to 1962, and 1998 to 2002 (based on the consecutive years when the smoothed reconstruction was below mean; Fig. 9a). The most severe July drought in the well-replicated portion of the reconstruction (after A.D. 664) is estimated to have occurred in the mid-thirteenth century, prior to and during Douglass's (1935) Great Drought among the Colorado Plateau Anasazi (Fig. 9b). This thirteenth-century July drought persisted for 45 yr (1245–89) but the most severe episode occurred from 1245 to 1252, including 1249, the driest reconstructed July from A.D. 664 to 2002 (Fig. 9b).

The episodic co-occurrence of cool- and warm-season drought (or wetness) over western New Mexico could magnify the environmental and socioeconomic impacts of decadal precipitation regimes and can be investigated

TABLE 2. Statistical properties of winter (November–May) and summer (July) precipitation observed and reconstructed for the average of New Mexico climate divisions 1 and 4 (northwest and west-central, respectively). Instrumental data obtained from the National Climatic Data Center.

a. Instrumental winter (Nov–May)

Period	*N*	Mean (mm)	Std dev (mm)	Skew	Kurtosis	Normal*
1931–2002	72	122.36	49.40	1.04	1.69	No
1960–2002	43	126.08	49.13	0.54	−0.30	Yes

b. Reconstructed winter (Nov–May)

Period	*N*	Mean (mm)	Std dev (mm)	Skew	Kurtosis	Normal*
b.c. 137–a.d. 2002	2139	121.65	35.79	0.24	−0.20	No
1931–2002	72	120.37	33.70	0.07	−0.97	Yes
1960–2002	43	126.08	32.76	0.00	−0.93	Yes

c. Instrumental summer (Jul)

Period	*N*	Mean (mm)	Std dev (mm)	Skew	Kurtosis	Normal*
1931–2004	72	48.74	16.64	0.43	−0.45	Yes
1960–2004	45	49.63	17.67	0.28	−0.46	Yes

d. Reconstructed summer (Jul)

Period	*N*	Mean (mm)	Std dev (mm)	Skew	Kurtosis	Normal*
b.c. 137– a.d. 2004	2141	48.96	14.78	1.82	6.29	No
1931–2004	74	48.65	12.52	1.95	4.88	No
1960–2004	45	49.72	13.49	2.10	5.42	No

* Shapiro–Wilk and Kolmogorov–Smirnov normality tests (SAS Institute 1985).

with the instrumental and reconstructed seasonal precipitation data. The instrumental and reconstructed data were first normalized:

$$\text{normalized } P_{\text{Nov-May}_t} = (P_{\text{Nov-May}_t} - \overline{X})(\text{sd}^{-1}) \quad \text{and} \quad (3)$$

$$\text{normalized } P_{\text{July}_t} = (P_{\text{July}_t} - \text{median})(\text{IQR}^{-1}), \quad (4)$$

where P is precipitation (either November–May total or July total, in year t), $\overline{X}$ is the mean and sd is the standard deviation of the November–May precipitation time series, and *median* is the 50th percentile and IQR is the interquartile range of the July precipitation time series (i.e., 75th–25th percentile).

The normalized instrumental precipitation data for each season are plotted in Fig. 10a and illustrate episodes of simultaneous cool- and early-warm-season drought and wetness from 1931 to 2005. Simultaneous interseasonal drought was persistent during the extended 1950s drought, but simultaneous pluvial conditions occurred only sporadically in this record (Fig. 10a). Most of these episodes of simultaneous drought or wetness are reproduced with the reconstructed cool- and early-warm-season estimates (not shown).

The simultaneous cool- and early-warm-season drought during the 1950s (Fig. 10a) is evident in the smoothed reconstructed series and is estimated to have been one of the most severe episodes of synchronous interseasonal drought in the past millennium (Fig. 11a). These interseasonal droughts can be referred to as perfect droughts because droughts during both the winter–spring and early summer growing season are unfavorable for first the germination and then the maturation and yield of dry-land crops such as maize (Benson et al. 2006). Simultaneous wet conditions in both seasons would favor enhanced dry-land crop yields (i.e., perfect pluvials). The two most severe and sustained episodes of simultaneous drought are estimated to have occurred in the eighth- and sixteenth-century megadroughts (Fig. 11a). Both cool- and early-warm-season precipitation reconstructions were below average during these events, but the winter–spring droughts appear to have been most extreme.

Simultaneous cool- and early-warm-season drought is estimated to have prevailed during the mid-seventeenth century (1657–73; Fig. 11a), when historical evidence indicates drought, famine, and disease among Pueblo and Spanish colonial societies in the Rio Grande region of New Mexico (Schroeder 1968; Sauer 1980; Barrett 2002; Cook et al. 2007; Stahle and Dean 2009). The seventeenth-century drought has been suggested as a potential analog for the impact of prolonged drought on prehistoric Anasazi societies (Stahle and Dean 2009), and the new reconstructions indicate that simultaneous

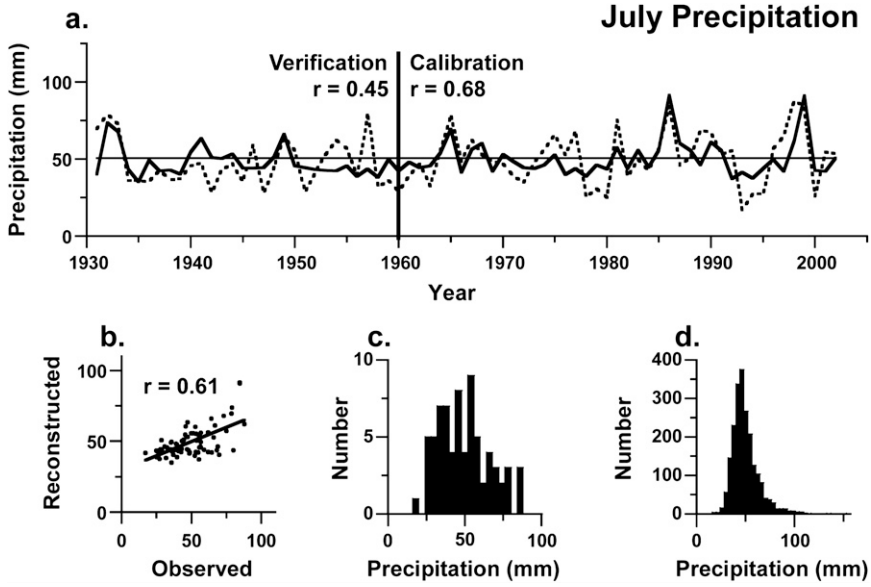

FIG. 8. (a) A time series comparison between observed (dashed line) and reconstructed (solid line) July precipitation for New Mexico climate divisions 1 and 4 (1931–2002). The reconstruction was based on the adjusted LW width chronology and was calibrated on the 1960–2002 period and verified by comparison with the instrumental data from 1931 to 1959. (b) The scatterplot between observed and reconstructed July precipitation. The frequency distributions of (c) observed and (d) reconstructed July precipitation (statistics in Table 2).

interseasonal drought occurred during part of the late-thirteenth-century Great Drought (Fig. 11a). Simultaneous drought conditions of the late-thirteenth century were not as severe as estimated for the mid-seventeenth century, but the smoothed cool- and warm-season reconstructions were both below normal from 1282 to 1289 and 1296 to 1298 (Fig. 11a), which may have been among the years of greatest environmental stress to the Anasazi subsistence system during the late-thirteenth century.

Drought has been implicated in the abandonment of the Anasazi great houses in the San Juan basin during the mid-twelfth century (Benson et al. 2006). Tree-ring-dated construction and remodeling of the great houses ended by A.D. 1130, including at Chaco Canyon and Aztec, apparently contemporaneous with a period of tree-ring-reconstructed cool-season drought conditions (Benson et al. 2006). The new winter–spring reconstruction from El Malpais, just south of the San Juan basin, confirms cool-season drought from A.D. 1125 to 1155, but simultaneous July drought was very limited during the mid-twelfth century (Figs. 9, 11a). However, one of the most persistent episodes of simultaneous cool- and early-warm-season drought is reconstructed for the late-twelfth century (Fig. 11a).

These new seasonal precipitation reconstructions do not provide strong support for the hypothesis that severe warm-season drought occurred simultaneously with dry winter–spring conditions during the mid-twelfth and late-thirteenth centuries and impacted the germination, maturation, and yield of dry-land maize crops, which are believed to have been essential to the Anasazi subsistence system (Benson et al. 2006). The simultaneous interseasonal droughts reconstructed for brief periods during the mid-twelfth and late-thirteenth centuries are suggestive of poor crop yields, but July precipitation is not correlated with August or September precipitation over northwestern New Mexico (based on the instrumental precipitation data from 1931 to 2005) and it is possible that late rains may have helped mitigate cool- and early-warm-season drought during some off the tree-ring-reconstructed droughts of the Anasazi era. Until it is possible to reconstruct precipitation for the full summer growing season from a spatially representative network of LW chronologies across the Colorado Plateau, the role of interseasonal drought on Anasazi agriculture will remain in question.

b. Asynchronous cool- and early-warm-season drought

The instrumental data also indicate years when cool- and early-warm-season precipitation were distinctly out of phase. Wet winter–spring conditions that were followed by dry Julys occurred in the 1930s and episodically after 1978, implying a late monsoon if not a poor monsoon season overall (Fig. 10b). Alternatively, dry

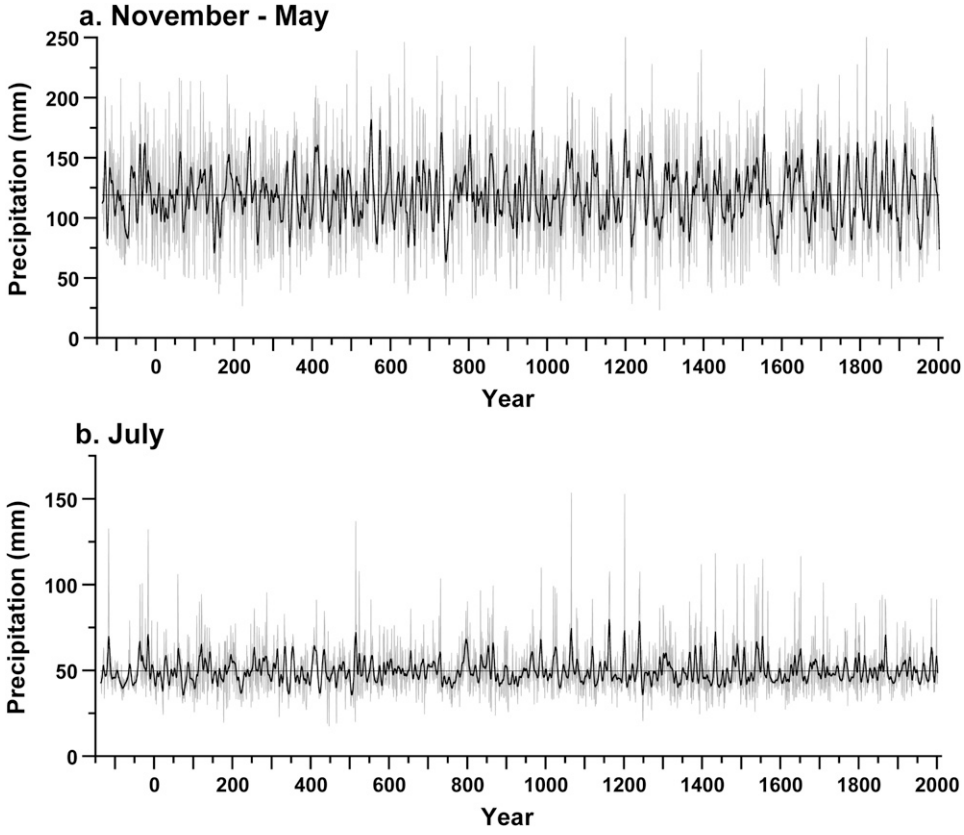

FIG. 9. (a) Winter–spring (November–May) and (b) July precipitation for New Mexico climate divisions 1 and 4 reconstructed from 137 B.C. to A.D. 2002 with the El Malpais EW and LW_{adj} width chronologies, respectively, each fitted with a cubic-smoothing spline designed to highlight decadal variability (black curves; Cook and Peters 1981).

winter–spring conditions followed by wet Julys, suggesting early monsoon onset, have been less prominent and persistent than the late monsoon condition in both the instrumental and smoothed reconstructed series (Figs. 10b, 11b, respectively). The cool- and early-warm-season precipitation data are not correlated for either the instrumental or reconstructed series, so the apparent phasing and antiphasing between these seasons may arise purely by chance. Nevertheless, the episodes of out-of-phase cool- and warm-season precipitation regimes might also involve a change in the large-scale ocean–atmospheric forcing of precipitation over the Southwest from the cool to early-warm season (Castro et al. 2007), a negative land surface feedback that has been hypothesized to influence the onset and intensity of the Southwest monsoon (Gutzler 2000), or perhaps both (see section 5d).

The episodes of asynchronous cool- and early-warm-season precipitation evident in the instrumental precipitation data during the twentieth century (Fig. 10b) are also present in the reconstructed series (not shown), but out-of-phase seasonal precipitation regimes appear to have been more common prior to 1630 in the smoothed reconstructions (Fig. 11b). The apparent decrease in the frequency of asynchronous cool- and early-warm-season precipitation regimes after the 1630s might be an artifact of the tree-ring sampling or failure to remove all biological growth persistence between the EW and LW chronologies. The cool- and early-warm-season reconstructions are not correlated on an interannual basis, but there is a weak positive correlation between the smoothed versions ($r = 0.43$ from 137 B.C. to A.D. 2002, which increases to $r = 0.61$ for 1630–2002). A more representative network of EW and LW chronologies across the North American monsoon region is currently under development and should provide a more robust long-term perspective on the phasing between reconstructed cool- and early-warm-season precipitation.

c. Ocean–atmospheric forcing of winter and summer precipitation

Correlation analyses of the global SST field illustrate the importance of the equatorial Pacific for winter–spring precipitation extremes over New Mexico (Fig. 12).

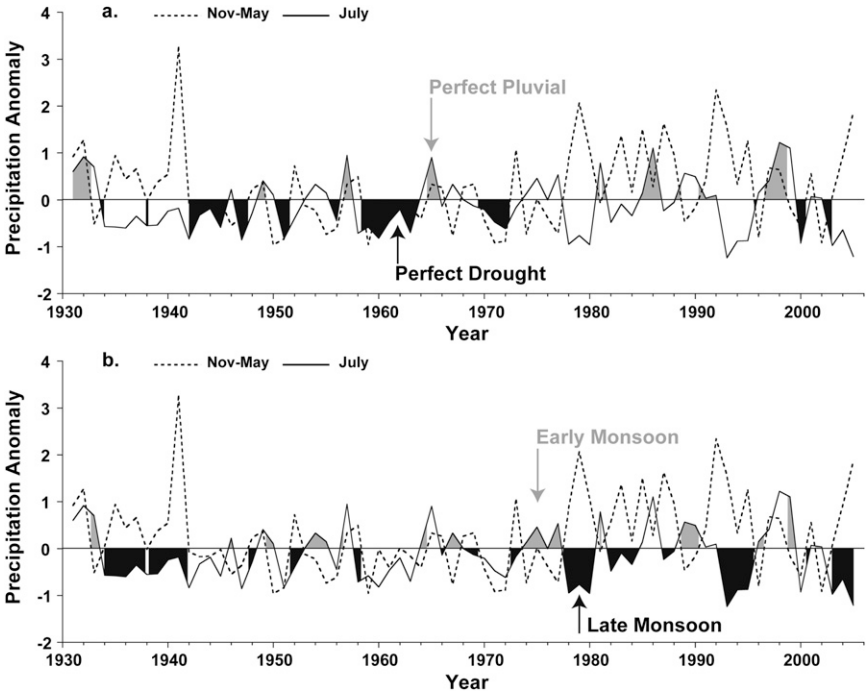

FIG. 10. (a) The instrumental cool- and early-warm-season (November–May and July, respectively) precipitation data for New Mexico divisions 1 and 4 have been normalized and periods of simultaneous cool- and early-warm-season drought (perfect interseasonal drought; black shading) and pluvial (perfect interseasonal pluvial; gray shading) are highlighted. (b) Episodes of antiphasing between normalized cool- and early-warm-season precipitation are highlighted and indicate early monsoon onset when the cool season was dry and July was wet and late monsoon onset when the cool season was wet and July was dry. These inferred early and late monsoons are in good agreement with the index of monsoon onset over Arizona and New Mexico available from 1963 to 1994 (Higgins et al. 1997).

The instrumental and reconstructed winter precipitation data for New Mexico were correlated with seasonalized SSTs [December–May (DJFMAM)] at 155 grid points between 70°N and 70°S (from Kaplan et al. 1997). The correlation coefficients were then mapped and the spatial SST patterns linked with winter precipitation anomalies over New Mexico are illustrated in Figs. 12a,b. El Niño conditions with warm SSTs in the eastern tropical and northeast Pacific, along with cool SSTs in the central North Pacific, are correlated with wet winters over New Mexico in both the instrumental and reconstructed data (Figs. 12a,b). The SST anomaly patterns are stronger using the instrumental rather than reconstructed data but the large-scale spatial patterns are remarkably similar.

Correlation analyses between anomalies in the 500-mb height field and observed winter–spring precipitation over New Mexico indicates negative correlations over the subtropics of the eastern North Pacific and North America and positive correlations over midlatitude North America (Figs. 12e,f). The negative correlations over the eastern North Pacific, in particular, are consistent with a recurrent trough in the 500-mb surface and with the warm SSTs in Figs. 12a,b. Given the warm El Niño–like conditions indicated by the correlation patterns in Fig. 12a, a recurrent subtropical jet would tend to enhance the influx of energy and moisture into southwestern North America, favoring cool-season precipitation over New Mexico. The same patterns, somewhat degraded, are evident in the SST and 500-mb correlations of reconstructed winter–spring precipitation over New Mexico (Figs. 12b,f), and these patterns are consistent with the PNA pattern of mid- to upper-tropospheric geopotential height anomalies over North America and the North Pacific during an El Niño event (Horel and Wallace 1981).

Summer precipitation over the Southwest, including July precipitation during the onset phase of the NAMS, has been linked with SSTs and circulation over the Pacific (Higgins et al. 1997; Higgins and Shi 2000; Castro et al. 2007), with the strength and position of the subtropical ridge over North America during summer (e.g., Carleton et al. 1990) and antecedent precipitation and snow cover over western North America (Gutzler 2000).

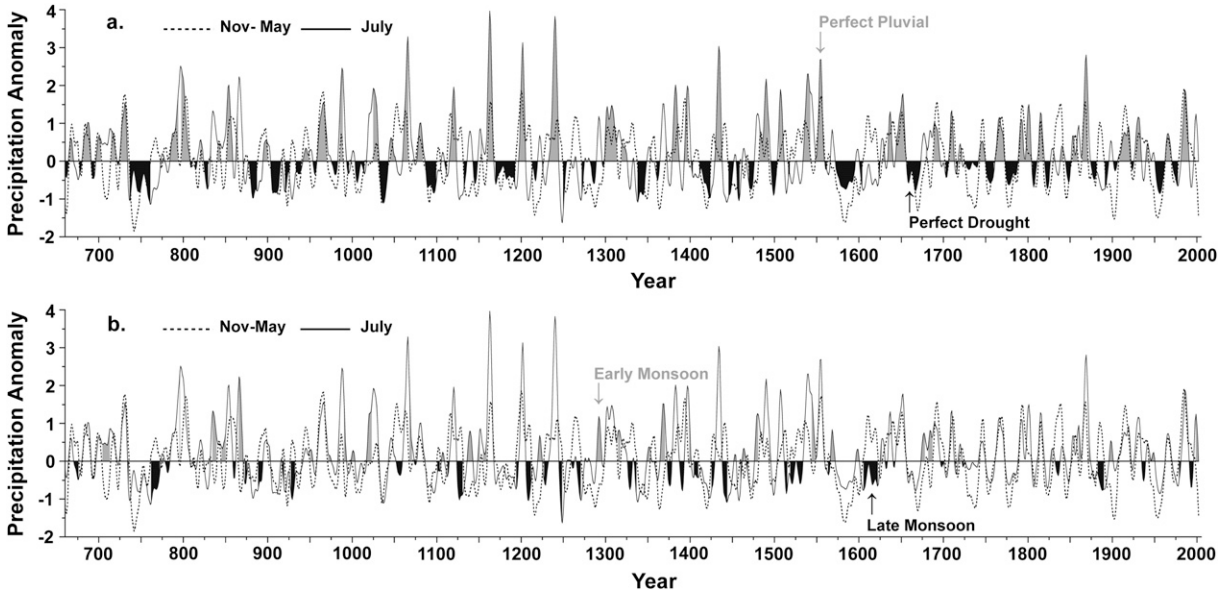

FIG. 11. As in Fig. 10, but the reconstructed cool- and early-warm-season precipitation series have been normalized and smoothed to emphasize decadal variability after A.D. 660, when the reconstructions are well replicated. (a) Note the episodes of simultaneous interseasonal drought (perfect drought; black shading), especially the 1950s, late-sixteenth, and mid-eighth centuries. The late-thirteenth-century Great Drought among the Colorado Plateau Anasazi included short episodes of simultaneous cool- and warm-season drought but not as severe or sustained as estimated during the mid-seventeenth-century Pueblo drought. Simultaneous cool- and early-warm-season wetness (perfect pluvial; gray shading) is estimated to have occurred throughout this smoothed record, persistently during the early-fourteenth, mid-sixteenth, mid-seventeenth, and early-twentieth centuries. (b) Note also the distinctly out-of-phase precipitation regimes in the early-seventeenth century, when wet winters were associated with dry conditions in July and presumably late onset of the monsoon. The opposite phasing, implying early monsoon onset, is less common in these reconstructions but is estimated during the late-thirteenth century and for other short episodes over the past 1300 yr.

Castro et al. (2001) have developed a conceptual model for the hemispheric-scale synoptic conditions associated with wet and dry summer monsoons over the southwestern United States, emphasizing moisture anomalies during the onset phase of June and July. Wet conditions during onset tend to be associated with cold SSTs in the eastern North Pacific, warm SSTs in the central North Pacific (i.e., the low phase of the PDO with a weak Aleutian low), La Niña conditions, and a strong ridge over western North America. The opposite conditions prevail in their model of dry conditions early in the Southwest monsoon season (Castro et al. 2001). Subsequently, Castro et al. (2007) have identified a combination of the interannual and interdecadal SST anomaly patterns over the Pacific during the boreal summer as most strongly teleconnected with the onset of the monsoon over the Southwest.

Correlation analyses with the global SST and 500-mb height fields were used to identify ocean–atmospheric signals in the observed and reconstructed July precipitation data for New Mexico during the instrumental era. The July precipitation series for New Mexico were correlated with a June plus July seasonalization of the Kaplan et al. (1997) gridded SST dataset, and the SST anomaly patterns are illustrated in Figs. 12c,d. These SST correlation patterns are not as strong as computed during the cool season, but the large-scale SST anomaly patterns implied by these correlations are very similar to the winter patterns (Figs. 12) and the sign of the precipitation response in July is reversed [as suggested by Castro et al. (2001) on decadal time scales]. In both the instrumental and reconstructed data, the cold North Pacific SST anomalies observed during wet July conditions (Figs. 12c,d) are consistent with a weak Aleutian low that would favor a long-wave trough over the eastern North Pacific and the monsoon ridge over North America that would lead to moisture advection into the Southwest at all levels and tend to enhance development of the NAMS (Carleton et al. 1990; Castro et al. 2001).

Correlation analyses with the 500-mb height field during June and July (Figs. 12g,h) resemble the circulation conditions over North America inferred from the SST anomalies associated with New Mexico precipitation. These analyses indicate that observed and reconstructed July precipitation over New Mexico are both positively correlated with 500-mb height anomalies over the subtropical North Pacific and over central and eastern North America. They are negatively correlated

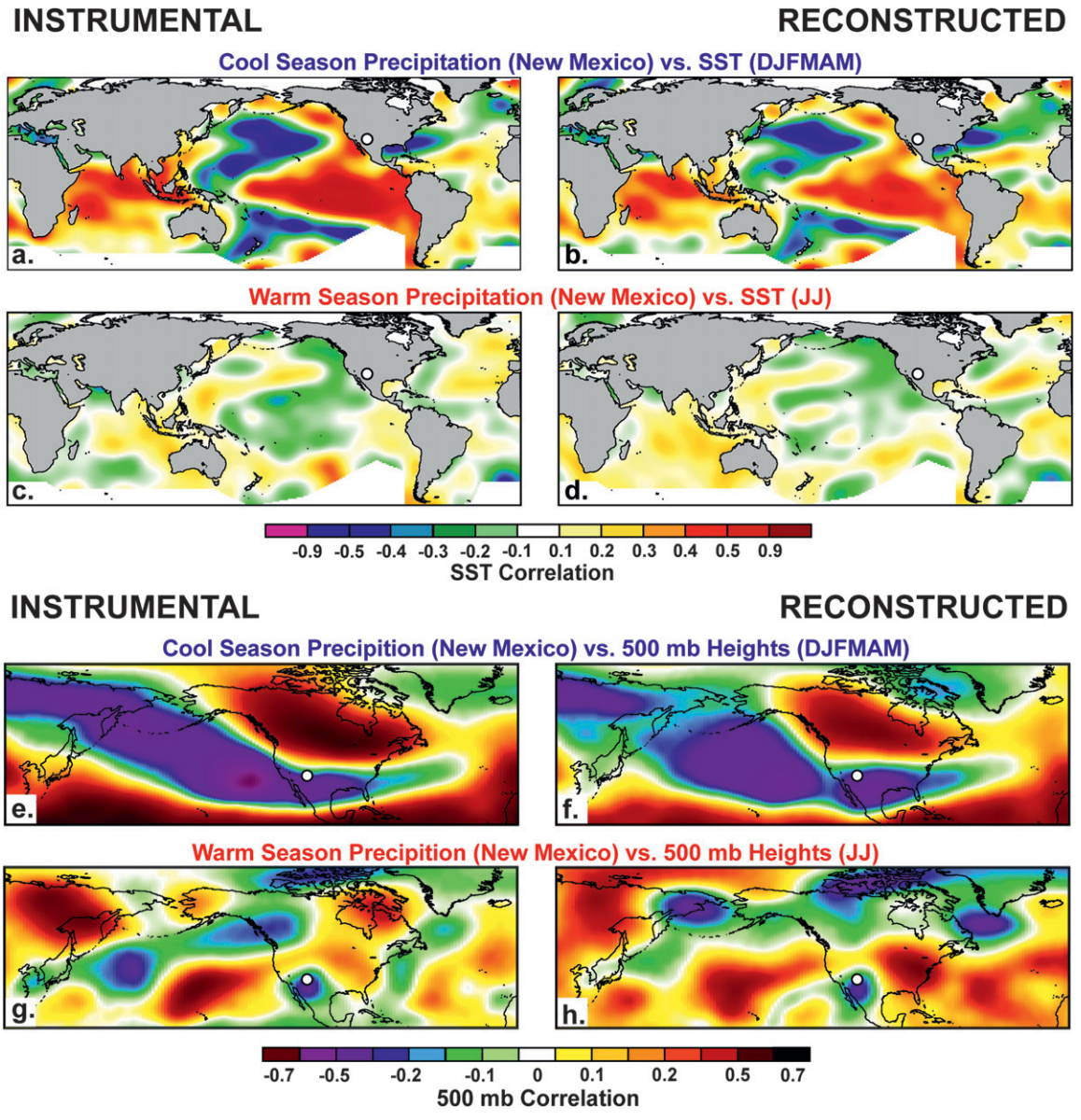

FIG. 12. The (a) instrumental and (b) reconstructed cool-season precipitation data for New Mexico divisions 1 and 4 (white dot; November–May totals) were correlated with global SST data from 1931 to 2002 (Kaplan et al. 1997), after the SSTs were averaged at each grid point to the winter–spring season (DJFMAM). Note the positive correlation with SSTs in the central and eastern tropical Pacific and the symmetrical negative correlations with midlatitude SSTs in the North and South Pacific for both the instrumental and reconstructed precipitation series. (c) Instrumental and (d) reconstructed July precipitation totals are correlated with June and July averaged SSTs. The summer SST correlations are much weaker but still quite consistent for the instrumental and reconstructed series. Note the gradient from positive to negative correlations from the central to northeastern North Pacific in both (c) and (d). The cool- and warm-season SST anomaly patterns implied by these correlations are similar but opposite in sign. (e)–(h) As in (a)–(d), but using the gridded 500-mb height anomaly data from 1948 to 2002 (NOAA reanalysis data, e.g., Kalnay et al. 1996). The consistency between the (a)–(d) SST and (e)–(h) 500-mb correlation maps for the instrumental and reconstructed data provides strong evidence that the tree-ring reconstructions of cool- and warm-season precipitation register both the interannual variability of regional precipitation and the large-scale ocean–atmospheric dynamics responsible for much of that variability.

with height anomalies over the monsoon region of northwestern Mexico and the southwestern United States (Figs. 12g,h). These 500-mb correlation patterns are consistent with the conceptual model of Castro et al. (2001), although the ridge axis in Figs. 12g,h is shifted eastward into the central and eastern United States for these empirical comparisons with July precipitation in northwestern New Mexico. Low 500-mb heights over the Southwest tend to prevail during wet Julys over New Mexico for both the observed and reconstructed data (Figs. 12g,h). The distribution of 500-mb height anomalies inferred from Figs. 12g,h would favor moisture advection into New Mexico from the North Pacific, Gulf of California, and Gulf of Mexico for both the instrumental and reconstructed July precipitation data (especially the Gulf of Mexico, given the ridge axis over the central and eastern United States). The correlation analyses with the SST and 500-mb height fields indicate that the cool- and warm-season precipitation reconstructions, which are based on the single long EW and LW chronologies from El Malpais, provide credible proxies for regional precipitation and the large-scale ocean–atmospheric features responsible for interannual variability.

d. Large-scale and regional forcing of monsoon onset over the Southwest

Castro et al. (2007) demonstrate that a combination of interannual (ENSO) and interdecadal modes of SST variability across the Pacific during the boreal summer are teleconnected with July precipitation and monsoon onset over the core region of the NAMS. In fact, the July precipitation response to this pan-Pacific SST mode actually changes sign from the cool-season precipitation response, which might account for antiphasing detected in the instrumental and tree-ring-reconstructed cool- and early-warm-season precipitation over New Mexico (Figs. 10b, 11b). Antecedent winter–spring precipitation has also been identified as a potential mechanism in the modulation of subsequent monsoon rainfall over the southwestern United States (Gutzler 2000; Grantz et al. 2007). Persistent spring snow cover and/or premonsoon soil moisture may delay the summer land surface heating needed to establish the land–ocean thermal gradient that leads to circulation changes responsible for the onset of the summer monsoon over the Southwest. Winter–spring precipitation and snow cover may therefore constitute a negative land surface feedback on the summer monsoon, where wet winters favor a delay in monsoon onset and less early-monsoon-season precipitation. Gutzler (2000) identified a negative correlation between spring snowpack over the southern Rocky Mountains and subsequent July–August total precipitation over western New Mexico from 1961 to 1990. Grantz et al. (2007) report a significant delay in monsoon onset and a decrease in July rainfall in response to antecedent winter–spring wetness over the Southwest. Grantz et al. (2007) link the winter–spring moisture anomalies to SSTs over the tropical and North Pacific and suggest that these antecedent ocean and land surface conditions may provide a basis for long-lead forecasts of monsoon rainfall over the Southwest. However, the covariability between cool-season and subsequent summer precipitation does not appear to be stable over multidecadal time scales and may have been interrupted by large-scale circulation regimes favorable to persistent drought over the Southwest during both the winter and summer seasons (e.g., the PDO; Gutzler 2000). The reconstructed winter–spring and July precipitation series may offer some insight into the hypothesized inverse relationship between cool- and warm-season precipitation anomalies over New Mexico at both interannual and decadal time scales.

Winter–spring and July precipitation totals over western New Mexico (divisions 1 and 4) are not correlated using the 72-yr instrumental records or the 2139-yr reconstructions. Nevertheless, there were episodes of distinct antiphasing between cool- and early-warm-season precipitation regimes in the instrumental and reconstructed data (at annual and decadal time scales, respectively; Figs. 10b, 11b). There is also statistical evidence for antiphasing between cool and subsequent July precipitation extremes in the annually resolved reconstructions, which might reflect regional land surface and/or large-scale ocean–atmospheric forcing of seasonal precipitation over New Mexico.

The reconstructed winter–spring and July precipitation data were analyzed with a four-way contingency table in which each reconstruction was divided into equal quartiles (very wet, wet, dry, and very dry; Table 3). Very dry July conditions follow very wet winter–spring conditions more often than expected by chance, whereas wet Julys tend to follow very dry conditions during winter–spring (Table 3). Alternatively, in-phase interseasonal drought extremes are rare, such that very dry conditions in July occur far less than expected after a very dry winter and spring (Table 3).

These results do not appear to be sensitive to the method used to remove the physiological dependence of LW on prior EW growth. The LW_{adj} chronology used to reconstruct July precipitation was calculated as the residuals from a linear regression of LW on EW (Fig. 5; $R^2 = 0.36$). But when the LW_{adj} chronology is based on the residuals from a seventh-order polynomial fit between the LW and EW chronologies ($R^2 = 0.366$; not shown), these polynomial residuals also exhibit the significant negative associations listed in Table 3.

TABLE 3. A contingency table analysis comparing four equal-size categories of reconstructed winter–spring precipitation with four equal categories of reconstructed July precipitation in western New Mexico (with July contingent on winter–spring). The four categories are very wet, wet, dry, and very dry, representing the 0–25th, 26th–50th, 51th–75th, and 76th–100th percentiles of seasonal precipitation (2125 total cases, with 16 missing). The expected cell sizes were approximately 133. The actual cell groupings are listed. The computed χ^2 of 174.55 for 9 degrees of freedom is significant at $P < 0.0001$. Very dry July precipitation amounts occurred in 33.9% of the cases when November–May precipitation was very wet (180/531; 25% expected). Very dry Julys occurred in only 8.1% of the cases when November–May precipitation was very dry (43/533; 25% expected). Very wet Julys occurred in 31.8% of the cases when November–May conditions were also very wet, contrary to the antiphasing between cool- and early-warm-season precipitation and perhaps reflecting a stagnant circulation regime with persistent interseasonal precipitation or possibly even biological growth persistence between earlywood and latewood growth not fully removed in derivation of the adjusted latewood chronology.

Nov–May precipitation	Jul precipitation				
	Very wet	Wet	Dry	Very dry	Total
Very wet	169*	95	87*	180*	531
Wet	117	109	132	173*	531
Dry	109	129	156	136	530
Very dry	139	196*	155	43*	533
Tot	534	529	530	532	2125

* The most influential cell groupings.

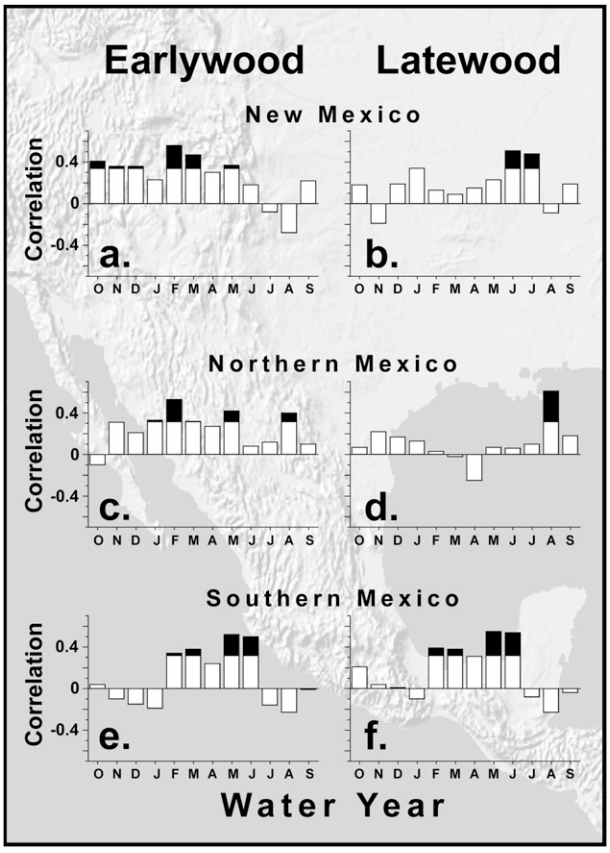

FIG. 13. Several 300–600-yr-long tree-ring chronologies of EW and LW width are now available for the monsoon region of North America [all Douglas-fir, ponderosa pine (*Pinus ponderosa*), or Montezuma baldcypress (*Taxodium mucronatum*)]. To estimate the regional precipitation response of these partial ring chronologies, regional average EW and LW_{adj} chronologies were computed in New Mexico, northern Mexico, and southern Mexico and each was correlated with monthly precipitation data for the area [climate divisions 1 and 4 in New Mexico, a five-station average in Durango, and the Hulme et al. (1998) grid point 4054 for southern Mexico]. The monthly responses for (a),(c),(e) EW and (b),(d),(f) LW [significant monthly correlations shaded black ($P < 0.05$)]. The EW and LW chronologies averaged for New Mexico were as follows: Spruce Canyon, CO; Ditch Canyon, Pueblita Canyon, El Malpais, Sunspot, and Guadalupe Peak, TX; for northern Mexico: Boot Springs (TX), Las Tinajas, El Tabacote, Creel, Canyon del Oro, Cerro Baraja, El Salto, and Rio Sabinas; and for southern Mexico: Villareal, Cuauhtemoc la Fragua, and Cerro la Pena.

The seasonal precipitation reconstructions provide new proxy evidence for monsoon onset over New Mexico. The short instrumental and long reconstructed seasonal precipitation series both suggest that inferred ''late monsoons'' have been more frequent and persistent than ''early monsoons'' (Figs. 10b, 11b). The reconstructions also indicate that decadal regimes of inferred early and late monsoons have both been subject to major changes in frequency of occurrence over the past 1300 yr (Fig. 11b). Development of an expanded array of cool- and warm-season precipitation reconstructions over the NAMS sector can test these preliminary observations and may provide deeper insight into the dynamics of the monsoon.

e. Potential for cool- and warm-season precipitation reconstruction over the monsoon region of North America

The El Malpais chronologies are currently the longest EW and LW chronologies available, but several shorter EW and LW chronologies have been completed for the monsoon region extending from the midlatitude Colorado Plateau into southern Mexico (e.g., Cleaveland 1986; Stahle et al. 2000b; Cleaveland et al. 2003; Villanueva-Diaz et al. 2007). Many of these chronologies provide discrimination among the seasonal precipitation regimes that dominate the climatology of this region and reflect distinctive climate dynamics. Figure 13 illustrates the seasonal climate signals recorded by EW and LW chronologies from selected conifer species across the region. The monthly precipitation signals recorded by the regionally averaged EW and LW_{adj} chronologies in New Mexico are clearly distinct (Figs. 13a,b). The New Mexican EW chronology responds to winter–spring precipitation (Fig. 13a), and the seasonalized November–May

precipitation total is correlated with the regional EW width chronology at +0.82 ($P < 0.001$), much stronger than the response of the single EW chronology from El Malpais. The regional LW_{adj} chronology is strongly correlated with precipitation in June and July ($r = 0.65$ and $P < 0.001$ for June+July total precipitation) and is not significantly correlated with winter–spring precipitation (Fig. 13b).

The discrimination between the seasonal climate response of EW and LW chronologies is also strong in the Sierra Madre Occidental of northern Mexico (Figs. 13c,d). The EW chronologies respond primarily to winter–spring precipitation (Fig. 13c) and the regional LW_{adj} is significantly correlated with August precipitation and lacks significant correlation with cool-season precipitation (Fig. 13d). The EW chronologies from northern Mexico are also strongly correlated with ENSO indices (Cleaveland et al. 2003), and the LW chronologies are linked with the NAMS (Therrell et al. 2002). There is little distinction between the EW and LW (or LW_{adj}) chronologies from southern Mexico (Figs. 13e,f), although the lack of high-quality monthly climate data in reasonable proximity to these remote upper-elevation collection sites makes the modeling of seasonal climate challenging. Nevertheless, the EW and LW chronologies from southern Mexico are both most strongly correlated with precipitation during the first half of the bimodal summer rainfall regime, prior to the ''canicula'' (midsummer drought; Figs. 13e,f).

6. Summary and conclusions

Chronologies of earlywood and latewood width from the ancient conifers at El Malpais National Monument record discrete cool- and warm-season precipitation signals and contrasting large-scale ocean atmospheric forcing. The derived 2139-yr-long reconstructions of cool- (November–May) and early-warm-season (July) precipitation are among the longest yet calculated with tree rings from the Southwest and the first to separate a summer precipitation estimate from the integrated winter–spring moisture signal ubiquitous in the annual rings of Southwestern arid-site conifers. The two seasonal reconstructions exhibit different statistical properties and are not correlated on annual time scales. The most severe sustained droughts estimated in the winter–spring reconstruction for northwestern New Mexico occurred during the eighth and sixteenth centuries and were part of profound dry spells affecting much of western North America (e.g., Meko et al. 1995; Stahle et al. 2000a; Acuna-Soto et al. 2005). Severe July drought is estimated to have persisted during both the eighth- and sixteenth-century events, producing what may have been the two most protracted periods of ''perfect'' interseasonal drought in the past 1300 yr. Simultaneous cool- and early-warm-season drought is also reconstructed during the mid-seventeenth-century drought, which had a severe impact on Pueblo and Spanish societies in colonial-era New Mexico. Simultaneous cool- and early-warm-season drought appears to have occurred at times during the late-thirteenth-century ''Great Drought,'' which has long been implicated in the migrations of the pre-Hispanic Anasazi but does not appear to have been as severe as during the seventeenth-century event.

The reconstructed winter and summer precipitation series for northwestern New Mexico reproduce the large-scale ocean–atmospheric dynamics responsible for cool- and early-warm-season precipitation identified in analyses of modern instrumental data. These dynamics include ENSO forcing and the PNA pattern of atmospheric circulation during the cool season. The instrumental and reconstructed July precipitation series are both associated with summer SST anomalies in the North Pacific conducive to the development of a 500-mb ridge over central North America, a trough over southwestern North America, and moisture advection into the Southwest from the North Pacific, the Gulf of California, and the Gulf of Mexico. The spatial correlation patterns of July precipitation compared with summer SSTs are similar to the wintertime SST correlation patterns computed for cool-season precipitation over New Mexico, but the sign of the correlation is reversed between the seasons. Contingency table analyses of the 2139-yr-long reconstructions indicate that wet winter–spring seasons were followed by dry July conditions at a higher frequency than expected by chance. This is in direct contrast to the positive physiological persistence between EW and LW growth in trees and may reflect the change in seasonal precipitation response to large-scale SST forcing from the Pacific, the role of antecedent precipitation and land surface conditions in the onset of the monsoon over New Mexico, or perhaps some interaction among these hypothesized regional and large-scale influences.

Improved temporal and spatial estimates of winter and summer precipitation will be possible once the many tree-ring samples already collected, dated, and resting in archives can be remeasured and new EW and LW width chronologies developed for the longest highest-quality series. In fact, a network of partial ring chronologies is beginning to emerge for the NAMS region (e.g., Therrell et al. 2002; Villanueva-Diaz et al. 2007), and good segregation of the seasonal precipitation signal can be demonstrated for selected EW and LW_{adj} chronologies from the southwestern United States and northern

Mexico. The parallel variance and climate forcing between the instrumental and reconstructed seasonal precipitation series across this region proves the value of EW and LW width chronologies for investigating climate dynamics over western North America.

Acknowledgments. This research was supported by the National Science Foundation (Grants ATM-0400712 and ATM-0753399). We thank the National Park Service, El Malpais National Monument, for permission to conduct this research on the Monument and the University of Arizona Laboratory of Tree-Ring Research for access and assistance with research collections. We acknowledge the advice and assistance of two reviewers, as well as J. S. Dean, J. R. Edmondson, B. T. Burns, E. Cornejo Oviedo, L. Vasquez Salem, R. Acuna Soto, L. V. Benson, C. L. Castro, and G. H. West.

REFERENCES

Acuna Soto, R., D. W. Stahle, M. D. Therrell, S. Gomez Chavez, and M. K. Cleaveland, 2005: Drought, epidemic disease, and the fall of classic period cultures in Mesoamerica (AD 750-950). *Med. Hypotheses,* **65,** 405–409.

Adams, D. K., and A. C. Comrie, 1997: The North American monsoon. *Bull. Amer. Meteor. Soc.,* **78,** 2197–2213.

Barrett, E. M., 2002: *Conquest and Catastrophe: Changing Rio Grande Pueblo Settlement Patterns in the Sixteenth and Seventeenth Centuries*. University of New Mexico Press, 180 pp.

Benson, L. V., 2003: Western lakes. *The Quaternary Period in the United States,* A. Gillespie, S. C. Porter, and B. Atwater, Eds., Developments in Quaternary Science, Vol. 1, Elsevier, 185–204.

——, K. Petersen, and J. Stein, 2006: Anasazi (pre-Columbian Native American) migrations during the middle-12th and late-13th centuries—Were they drought induced? *Climatic Change,* **83,** 187–213.

——, M. S. Berry, E. A. Jolie, J. D. Spangler, D. W. Stahle, and E. M. Hattori, 2007: Possible impacts of early-11th-, middle-12th-, and late-13th-century droughts on western Native Americans and the Mississippian Cahokians. *Quat. Sci. Rev.,* **26,** 336–350.

Biondi, F., A. Gershunov, and D. R. Cayan, 2001: North Pacific decadal climate variability since AD 1661. *J. Climate,* **14,** 5–10.

Burns, B. T., 1983: Simulated Anasazi storage behavior using crop yields reconstructed from tree rings: AD 652-1968. Ph.D. dissertation, University of Arizona, 756 pp.

Carleton, A. M., 1987: Summer circulation climate of the American Southwest, 1945–1984. *Ann. Assoc. Amer. Geogr.,* **77,** 619–634.

——, D. A. Carpenter, and P. J. Weser, 1990: Mechanisms of interannual variability of the Southwest United States summer rainfall maximum. *J. Climate,* **3,** 999–1015.

Castro, C. L., T. B. McKee, and R. A. Pielke Sr., 2001: The relationship of the North American monsoon to tropical and North Pacific sea surface temperatures as revealed by observational analyses. *J. Climate,* **14,** 4449–4473.

——, R. A. Pielke Sr., J. O. Adegoke, S. D. Schubert, and P. J. Pegion, 2007: Investigation of the summer climate of the contiguous United States and Mexico using the Regional Atmospheric Modeling System (RAMS). Part II: Model climate variability. *J. Climate,* **20,** 3866–3887.

Cleaveland, M. K., 1975: Dendroclimatic relationships of shortleaf pine (*Pinus echinata* Mill.) in the South Carolina Piedmont. M.S. thesis, Dept. of Forestry, Clemson University, 189 pp.

——, 1983: X-ray densitometric measurement of climatic influence on the intra-annual characteristics of southwestern semiarid conifer tree rings. Ph.D. dissertation, University of Arizona, 177 pp.

——, 1986: Climatic response of densitometric properties in semiarid site tree rings. *Tree-Ring Bull,* **46,** 13–29.

——, D. W. Stahle, M. D. Therrell, J. Villanueava-Diaz, and B. T. Burns, 2003: Tree-ring reconstructed winter precipitation in Durango, Mexico. *Climatic Change,* **59,** 369–388.

Cook, E. R., 1985: A time series analysis approach to tree-ring standardization. Ph.D. dissertation, University of Arizona, 171 pp.

——, and K. Peters, 1981: The smoothing spline: A new approach standardizing forest interior tree-ring series for dendroclimatic studies. *Tree-Ring Bull.,* **41,** 45–53.

——, and R. L. Holmes, 1986: Users manual for program ARSTAN. *Chronology*, series VI, University of Arizona, 182 pp.

——, and L. A. Kairiukstis, Eds., 1990: *Methods of Dendrochronology: Applications in the Environmental Sciences*. Kluwer, 394 pp.

——, C. Woodhouse, C. M. Eakin, D. M. Meko, and D. W. Stahle, 2004: Long-term aridity changes in the western United States. *Science,* **306,** 1015–1018.

——, R. Seager, M. A. Cane, and D. W. Stahle, 2007: North American drought: Reconstructions, causes, and consequences. *Earth Sci. Rev.,* **81,** 93–134.

D'Arrigo, R. D., and G. C. Jacoby, 1991: A 1000-year record of winter precipitation from northwestern New Mexico, USA: A reconstruction from tree rings and its relation to El Niño and the Southern Oscillation. *Holocene,* **1,** 95–101.

Douglas, M. W., R. A. Maddox, K. Howard, and S. Reyes, 1993: The Mexican monsoon. *J. Climate,* **6,** 1665–1677.

Douglass, A. E., 1920: Tree-ring evidence of past climatic variability. *Ecology,* **1,** 24–32.

——, 1935: *Dating Pueblo Bonito and Other Ruins of the Southwest*. National Geographic Society Contributed Technical Papers Pueblo Bonito Series, Vol. 1, National Geographic Society, 74 pp.

——, 1941: Crossdating in dendrochronology. *J. For.,* **39,** 825–828.

Draper, N. R., and H. Smith, 1981: *Applied Regression Analysis*. 2nd ed. John Wiley & Sons, 709 pp.

Fritts, H. C., 1966: Growth-rings of trees: Their correlation with climate. *Science,* **154,** 973–979.

——, 2001: *Tree Rings and Climate*. Blackburn Press, 567 pp.

Gedalof, Z., and D. J. Smith, 2001: Interdecadal climate variability and regime-scale shifts in Pacific North America. *Geophys. Res. Lett.,* **28,** 1515–1518.

Grantz, K., B. Rajagopalan, M. Clark, and E. Zagona, 2007: Seasonal shifts in the North American monsoon. *J. Climate,* **20,** 1923–1935.

Grissino-Mayer, H. D., 1995: Tree-ring reconstructions of climate and fire history at El Malpais National Monument, New Mexico. Ph.D. dissertation, University of Arizona, 407 pp.

——, 2001: Assessing crossdating accuracy: A manual and tutorial for the computer program COFECHA. *Tree-Ring Res.,* **57,** 205–221.

——, T. W. Swetnam, and R. K. Adams, 1997: The rare, old-aged conifers of El Malpais—Their role in understanding climatic change in the American Southwest. *N. M. Bur. Mines Miner. Res. Bull.,* **156,** 155–161.

Gutzler, D. S., 2000: Covariability of spring snowpack and summer rainfall across the southwest United States. *J. Climate,* **13,** 4018–4027.

Herweijer, C., R. Seager, and E. R. Cook, 2006: North American droughts of the mid to late nineteenth century: A history, simulation, and implication for mediaeval drought. *Holocene,* **16,** 159–171.

Hidalgo, H. G., T. C. Piechota, and J. A. Dracup, 2000: Stream flow reconstruction using alternative PCA-based regression procedures. *Water Resour. Res.,* **36,** 3241–3249.

Higgins, R. W., and W. Shi, 2000: Dominant factors responsible for interannual variability of the summer monsoon in the southwestern United States. *J. Climate,* **13,** 759–776.

——, Y. Yao, and X. Wang, 1997: Influence of the North American monsoon system on the U.S. summer precipitation regime. *J. Climate,* **10,** 2600–2622.

——, Y. Chen, and A. V. Douglas, 1999: Interannual variability of the North American warm season precipitation regime. *J. Climate,* **12,** 653–680.

Holmes, R. L., 1983: Computer-assisted quality control in tree-ring dating and measurement. *Tree-Ring Bull.,* **44,** 69–78.

Horel, J. D., and J. M. Wallace, 1981: Planetary-scale atmospheric phenomena associated with the Southern Oscillation. *Mon. Wea. Rev.,* **109,** 813–829.

Hulme, M., T. J. Osborn, and T. C. Johns, 1998: Precipitation sensitivity to global warming: Comparisons of observations with HadCM2 simulations. *Geophys. Res. Lett.,* **25,** 3379–3382.

Kalnay, E., and Coauthors, 1996: The NCEP/NCAR 40-Year Reanalysis Project. *Bull. Amer. Meteor. Soc.,* **77,** 437–471.

Kaplan, A., M. A. Cane, Y. Kushnir, A. C. Clement, M. B. Blumenthal, and B. Rajagopalan, 1998: Analyses of global sea surface temperature 1856–1991. *J. Geophys. Res.,* **103,** 27 835–27 860.

Karl, T. R., L. K. Metcalf, M. L. Nicodemus, and R. G. Quayle, 1983: Statewide average climatic history, New Mexico 1895-1983. *Historical Climatology Series,* Vol. 6-1, National Climatic Data Center, 35 pp.

Lindsey, A. A., 1951: Vegetation and habitats in a southwestern volcanic area. *Ecol. Monogr.,* **21,** 227–253.

Lough, J. M., and H. C. Fritts, 1985: The Southern Oscillation and tree rings: 1600–1961. *J. Climate Appl. Meteor.,* **24,** 952–966.

Meko, D. M., and C. H. Baisan, 2001: Pilot study of latewood-width of conifers as an indicator of variability of summer rainfall in the North American monsoon region. *Int. J. Climatol.,* **21,** 697–708.

——, C. W. Stockton, and W. R. Boggess, 1980: A tree-ring reconstruction of drought in southern California. *Water Resour. Bull.,* **16,** 594–600.

——, ——, and ——, 1995: The tree-ring record of severe sustained drought. *Water Resour. Bull.,* **31,** 789–801.

——, C. A. Woodhouse, C. A. Baisan, T. Knight, J. J. Lukas, M. K. Hughes, and M. W. Salzer, 2007: Medieval drought in the upper Colorado River Basin. *Geophys. Res. Lett.,* **34,** L10705, doi:10.1029/2007GL029988.

Mitchell, D. L., D. Ivanova, R. Rabin, T. J. Brown, and K. Redmond, 2002: Gulf of California sea surface temperatures and the North American monsoon: Mechanistic implications from observations. *J. Climate,* **15,** 2261–2281.

Nicholas, R. E., and D. S. Battisti, 2008: Drought recurrence and seasonal rainfall prediction in the Río Yaqui basin, Mexico. *J. Appl. Meteor. Climatol.,* **47,** 991–1005.

Panshin, A. J., and C. de Zeeuw, 1970: *Textbook of Wood Technology*. Vol. 1, McGraw-Hill, 705 pp.

Ropelewski, C. F., and M. S. Halpert, 1987: Global and regional scale precipitation patterns associated with the El Niño/Southern Oscillation. *Mon. Wea. Rev.,* **115,** 1606–1626.

Rose, M. R., J. S. Dean, and W. J. Robinson, 1981: *The Past Climate of Arroyo Hondo, New Mexico, Reconstructed from Tree Rings*. Arroyo Hondo Archaeological Series, Vol. 4, School of American Research Press, 1–114.

Salzer, M. W., and K. F. Kipfmueller, 2005: Reconstructed temperature and precipitation on a millennial timescale from tree rings in the southern Colorado Plateau. *Climatic Change,* **70,** 465–487.

SAS Institute, 1985: SAS User's Guide: Basics, Version 5 Edition. SAS Institute, Inc., 1290 pp.

Sauer, C. O., 1980: *Seventeenth Century North America*. Turtle Island, 295 pp.

Schroeder, A. H., 1968: Shifting for survival in the Spanish Southwest. *N. M. Hist. Rev.,* **43,** 291–310.

Schulman, E., 1942: Dendrochronology in pines of Arkansas. *Ecology,* **23,** 309–318.

——, 1945: Runoff histories in tree rings of the Pacific Slope. *Geogr. Rev.,* **36,** 59–73.

Seager, R., N. Harnik, Y. Kushnir, W. Robinson, and J. Miller, 2003: Mechanisms of hemispherically symmetric climate variability. *J. Climate,* **16,** 2960–2978.

——, Y. Kushnir, C. Herweijer, N. Naik, and J. Miller, 2005: Modeling of tropical forcing of persistent droughts and pluvials over western North America: 1856–2000. *J. Climate,* **18,** 4065–4088.

Sheppard, P. R., A. C. Comrie, G. D. Packin, K. Angersbach, and M. K. Hughes, 2002: The climate of the US Southwest. *Climate Res.,* **21,** 219–238.

Stahle, D. W., and J. S. Dean, 2009: North American tree rings, climatic extremes, and social disasters. *Dendroclimatology: Progress and Prospects,* M. K. Hughes, H. F. Diaz, and T. W. Swetnam, Eds., Developments in Paleoecological Research, Vol. 11, Springer, in press.

——, and Coauthors, 1998: Experimental dendroclimatic reconstruction of the Southern Oscillation. *Bull. Amer. Meteor. Soc.,* **79,** 137–152.

——, E. R. Cook, M. K. Cleaveland, M. D. Therrell, D. M. Meko, H. D. Grissino-Mayer, E. Watson, and B. H. Luckman, 2000a: Tree-ring data document 16th century megadrought over North America. *Eos, Trans. Amer. Geophys. Union,* **81,** 121.

——, and Coauthors, 2000b: Recent tree-ring research in Mexico. *Dendrocronología en América Latina*, F. Roig, Ed., EDIUNC, 285–306.

Steel, R. G. D., and J. H. Torrie, 1980: *Principles and Procedures of Statistics: A Biometrical Approach*. 2nd ed. McGraw-Hill, 633 pp.

Stockton, C. W., 1975: *Long-Term Streamflow Records Reconstructed from Tree Rings*. Vol. 5, *Papers of the Laboratory of Tree-Ring Research,* University of Arizona Press, 111 pp.

Stokes, M. A., and T. L. Smiley, 1996: *An Introduction to Tree-Ring Dating*. 2nd ed. University of Arizona Press, 73 pp.

Therrell, M. D., D. W. Stahle, M. K. Cleaveland, and J. Villanueva-Diaz, 2002: Warm season tree growth and precipitation over Mexico. *J. Geophys. Res.,* **107,** 4205, doi:10.1029/2001JD000851.

Villanueva-Diaz, J., D. W. Stahle, B. H. Luckman, J. Cerano-Paredes, M. D. Therrell, M. K. Cleaveland, and E. Cornejo-Oviedo, 2007: Winter-spring precipitation reconstruction from tree rings for northeast Mexico. *Climatic Change,* **83,** 117–131.

Wang, C., 2007: Variability of the Caribbean low-level jet and its relations to climate. *Climate Dyn.,* **29,** 411–422.

——, and D. B. Enfield, 2003: A further study of the tropical Western Hemisphere warm pool. *J. Climate,* **16,** 1476–1493.

Woodhouse, C. A., K. E. Kunkel, D. R. Easterling, and E. R. Cook, 2005: The twentieth-century pluvial in the western United States. *Geophys. Res. Lett.,* **32,** L07701, doi:10.1029/2005GL022413.

Zhang, Y., J. M. Wallace, and D. S. Battisti, 1997: ENSO-like interdecadal variability: 1900–93. *J. Climate,* **10,** 1004–1020.

Zhu, C., D. P. Lettenmaier, and T. Cavazos, 2005: Role of antecedent land surface conditions on North American monsoon rainfall variability. *J. Climate,* **18,** 3104–3121.